Supplementary Information

The levelized cost of exergy: a technoeconomic framework for energy system comparison

Jordan D. Kocher,[a,b,*] Aravindh Rajan,[c] Jason Woods,[a] Walter P. Parker Jr.,[a,b] Samuel Woolsey,[b] and Akanksha K. Menon[a,b,*]

[a]National Laboratory of the Rockies, Golden, CO, USA

[b]George W. Woodruff School of Mechanical Engineering, Georgia Institute of Technology, Atlanta, GA, USA

[c]Orca Sciences, Kirkland, WA, USA

*Corresponding author. Email: jordan.kocher@nrel.gov

*Corresponding author. Email: akanksha.menon@me.gatech.edu

Supplementary Note 1: CAPEX per Unit Exergy Output

The plot with three axes illustrated in Figure S1 can be used to find the LCOEx of the output of an energy system. A reverse osmosis plant is plotted as an example. The first contribution to the LCOEx of the output is the cost of exergy consumption, which is simply the LCOEx of the input (6 ¢/kWh_{ex} electricity in this example). The second contribution to the LCOEx of the system output is all costs other than the exergy input, which is represented by the "system ownership costs" axis (*i.e.*, plant CAPEX, and all OPEX not associated with the energy input, such as maintenance costs). The values on this axis are expressed per kWh_{ex} of the exergy input to the system (37 ¢/kWh_{ex} in this case). Adding the value from this axis to the LCOEx of the system input yields total system cost (CAPEX, energy OPEX, and all other OPEX) per unit exergy input; in this example, a value of 43 ¢/kWh_{ex} results. The final step in obtaining the LCOEx of the system output is to divide the total cost per exergy input by the exergetic efficiency of the system (0.33 in this example). Applying this methodology to the example in Figure S1, the LCOEx of the output comes out to be 130 ¢/kWh_{ex}. Multiplying by the volumetric exergy of fresh water, relative to the dead state of seawater (0.78 kWh_{ex}/m^3) yields the levelized cost of water (LCOW), which comes out to be approximately \$1/m^3, which is the industry standard for RO desalination.[1]

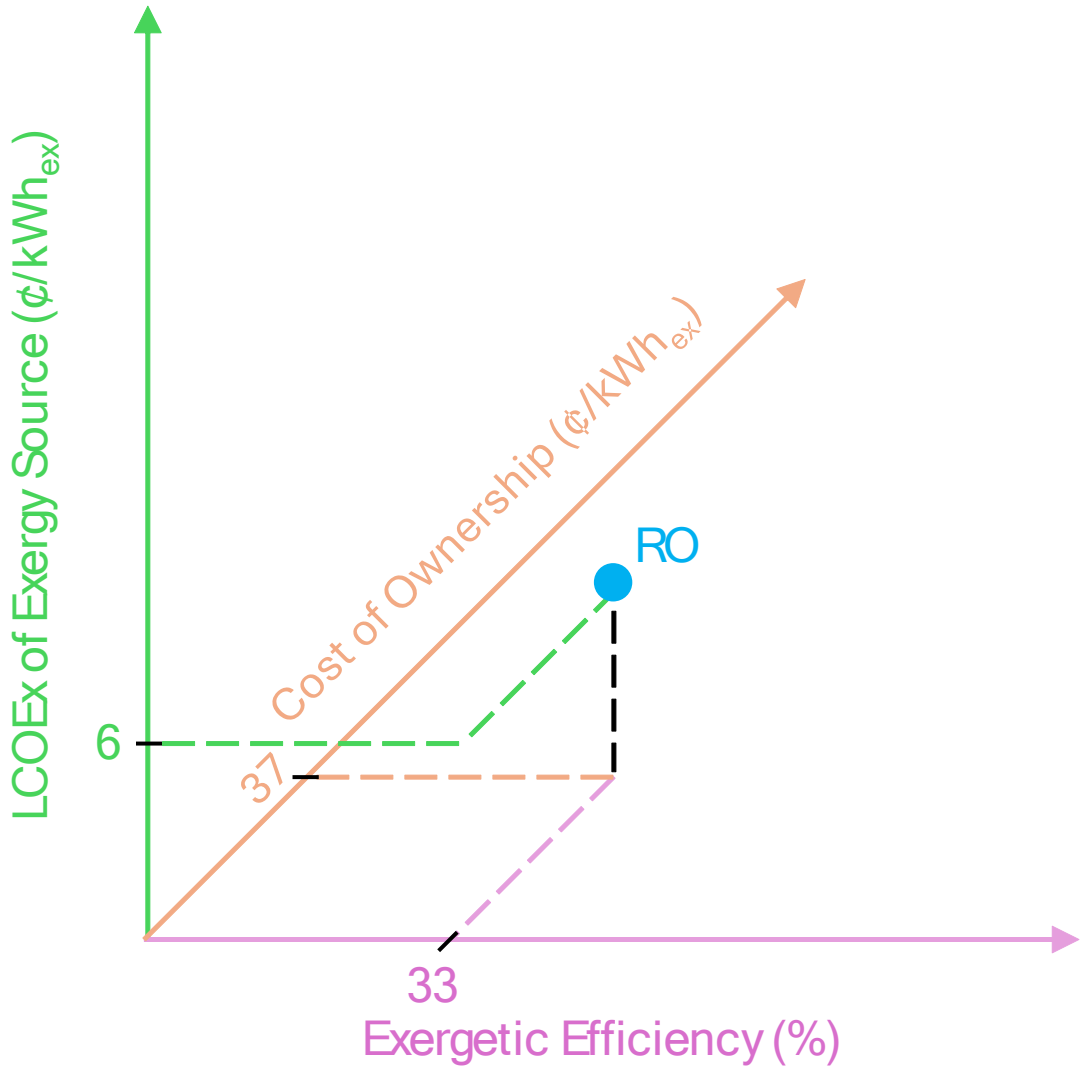

Figure S1. Regime map used to evaluate the LCOEx of a system's output, plotting the LCOEx of the system input (exergy source), exergetic efficiency of the system, and system ownership costs (*e.g.*, CAPEX).

To obtain the system ownership cost (*i.e.*, CAPEX and non-energy OPEX) on a per kWh_{ex} output basis, the following procedure is followed. First, the CAPEX is annualized by multiplying by the capital recovery factor (CRF); for a plant CAPEX of $20,000,000, a lifetime of 30 years, and a discount rate of 6.9%, the discount rate is 0.08 and the term CAPEX × CRF comes out to be $1,600,000/yr. To this number the annual OPEX (another $1,600,000/yr in this example) is added, yielding $3,200,000/yr. Then, this number is divided by the annual exergy consumption (*i.e.*, the

exergy input). In this example, we assume that the desalination plant has a capacity of 10,000 m^3 of water per day and operates 365 day per year. The volumetric exergy density of freshwater is 0.78 kWh_{ex}/m^3, to which the daily plant capacity and number of operational days per year are multiplied, yielding an annual exergy output of 2,847,000 kWh_{ex}/yr. Based on the exergetic efficiency of 0.33, the annual exergy input to the plant is 8,627,273 kWh_{ex}/yr. Thus, the plant ownership cost per unit exergy input comes out to be 37 ¢ per kWh_{ex} of electricity input. This is the number plotted on the system ownership cost axis in Figure S1. This number, along with the LCOEx of the energy input and the exergetic efficiency of the system, can also be used to draw the Sankey diagram for the LCOEx of the system output, as shown in Figure S2. The LCOEx Sankey diagram consists of two flows: the cost flow (top of Figure S2, in green) and the exergy flow (bottom of Figure S2, in yellow). The first flow in the cost portion is the LCOEx of the system input, in ¢; in this example, it is 6 ¢. Meanwhile, the first flow in the exergy portion of the Sankey diagram is always 1 kWh_{ex}, as all costs have been normalized per unit exergy input to the system. Then, the system ownership (*i.e.*, CAPEX and non-energy OPEX) serves as a cost source, which flows into the cost portion of the diagram; in this example, the system ownership cost is a source of 37 ¢. Finally, the exergetic efficiency must be accounted for in the exergy flow portion of the diagram. The exergy destruction serves as an exergy sink, and destroyed exergy flows out of the exergy portion of the diagram. Because the exergy input was chosen to be 1 kWh_{ex}, the amount of destroyed exergy is simply equal to one minus the exergetic efficiency. In this example, the exergy efficiency is 0.33, so 0.67 kWh_{ex} flows out of the exergy portion of the diagram due to exergy destruction. The LCOEx of the system output is then equal to the final cost flow (in ¢) divided by the final exergy flow (in kWh_{ex}), which, for this example, has a value of 130 ¢/kWh_{ex}.

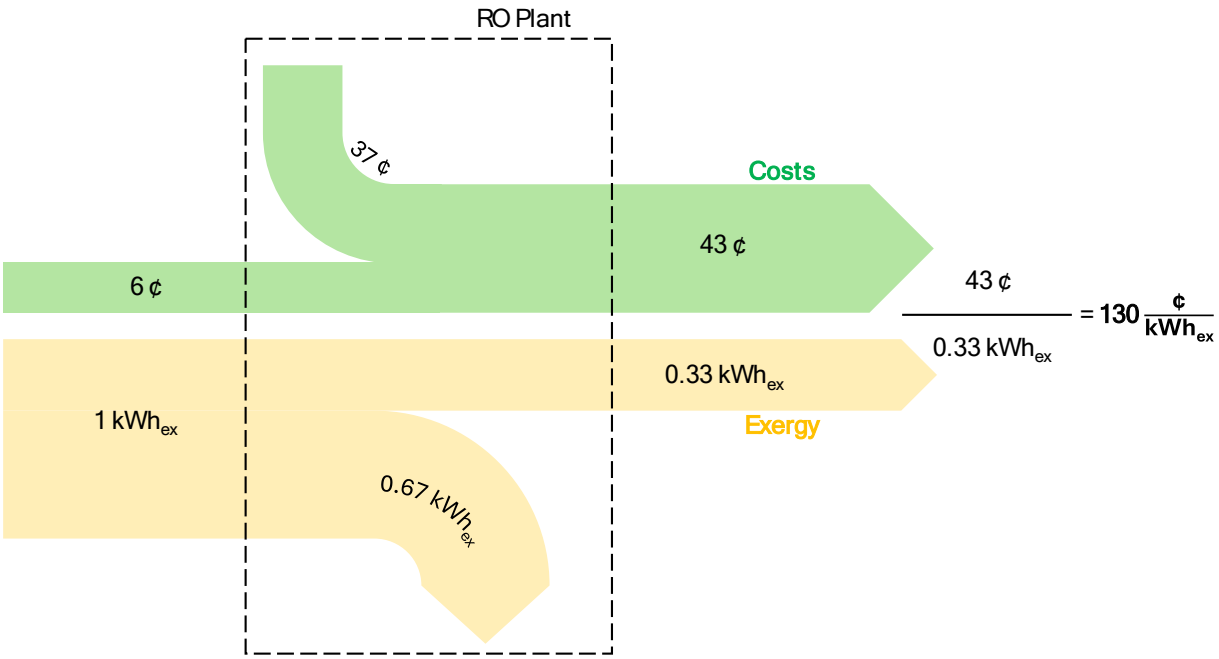

Figure S2. LCOEx Sankey diagram for an RO plant.

Supplementary Note 2: Analysis of the Flat Plate Collector

To simulate the flat plate solar collector, we used NREL's System Advisor Model (SAM). Table S1 below gives the list of inputs used for the analysis. In the simulation, the solar collector is connected to a water tank; we take the tank temperature as the temperature at which the collector provides exergy for each hour of the year (*i.e.*, the temperature of the thermal load).

Table S1. NREL SAM flat plate collector simulation inputs. Any inputs not listed were kept at their default values.

SAM Simulation Input	Value
Solar resource file	phoenix_az_33.450495_-111.983688_psmv3_60_tmy
Average daily hot water draw	Varied (1 to 1000 kg/day)
Tilt	33.4484 deg
Working fluid	Glycol
Number of collectors	1
Collector	Heliodyne Inc. Gobi 408 013
Solar tank loss coefficient	1e-05 W/m^2-K
Pipe insulation conductivity	1e-06 W/m-K

We varied the hot water usage and found the optimal flowrate at which the exergy delivered to the thermal load was maximized. For low usage, the temperature of heat delivery was high, but the rate of heat transfer was low. At high usage, the rate of heat transfer was high, but the temperature of heat delivery was low. At each usage value, the exergy delivered was calculated for each hour of the year, based on the hourly ambient temperature, water tank temperature, and rate of heat transfer (denoted as Q_{useful} in the SAM program). For the simulation inputs in Table S1, we found that the optimal hot water usage was ~ 50 kg/day; this yields an annual heat delivery of 301 kWh_{th}/m^2 per year and an annual exergy delivery of 41 kWh_{ex}/m^2 per year.

To calculate the LCOH and LCOEx of the flat plate collector, the financial parameters were taken from Menon *et al.*,[2] who used a CAPEX of 120/m^2 for low temperature collectors, annual OPEX of \$2.4/m^2 per year, a discount rate of 7%, and a collector lifetime of 20 years. This yields an annual cost of \$13.73/m^2 per year. From this cost, as well as the annual heat and exergy delivery calculated above, the LCOH is 4.56 ¢/kWh_{th}, while the LCOEx is 33.49 ¢/kWh_{ex}.

Supplementary Note 3: Analysis of the Black Pipe as a Solar Thermal Collector

To see if a heat source with a lower CAPEX would serve as an inexpensive exergy source, we consider an ultra-simple, very low-grade heat delivery source – a metal pipe painted black – in Figure S3. This heat source could, in theory, be used to provide heat to a variety of different systems; for example, systems using lower critical solution temperature mixtures to produce desalination,[3–5] atmospheric water harvesting,[6,7] dehumidification,[8] and refrigeration[8] with heat sources at temperatures ≤ 50 °C have recently been developed. As a particular example, we list the AWH application in Figure S3a, since many AWH prototypes powered by low-grade heat have been developed.[7,9,10] To analyze the performance of this heat source, the thermal resistance network in Figure S3b is used. We make several generous assumptions in this analysis, to see how this very low-grade heat source would perform under the best of conditions. First, when calculating LCOEx, we assume that natural convection occurs at the exterior tube surface instead of forced convection, without accounting for the cost of any sort of wind shield (results of the heat transfer analysis are given for both forced and natural convection, but only natural convection was considered when calculating LCOH and LCOEx). Second, the results in Figure S3 correspond to Phoenix, Arizona, a location with high solar irradiance. Third, we assume that the pipe is always turned to face the sun (without any energy consumption) so that the projected area facing the sun is maximized. For the areal cost of the pipe, we use a value of \$16.70/m^2, which is based on a cost of \$15.62/m^2 for the cost to produce a 1" outer diameter aluminum pipe and \$1.08/m^2 for the paint. Finally, most systems are designed to operate around a fixed heat source temperature (*e.g.*, the desorption temperature of a sorbent,[10] or the transition temperature of a thermally responsive mixture[6]). We find the optimal fixed heat delivery temperature that would minimize LCOEx, but we also provide results for the scenario where the heat delivery temperature is allowed to vary

between each time interval and the temperature that maximizes exergy delivered during the interval is selected. The results in Figure S3 were generated using direct normal irradiance, air temperature, and wind speed data from NREL's National Solar Radiation Database (NSRDB) for the year 2013. For the CAPEX, we assume a discount rate of 7% and a pipe lifetime of 50 years, with zero operating expenses (another favorable assumption).

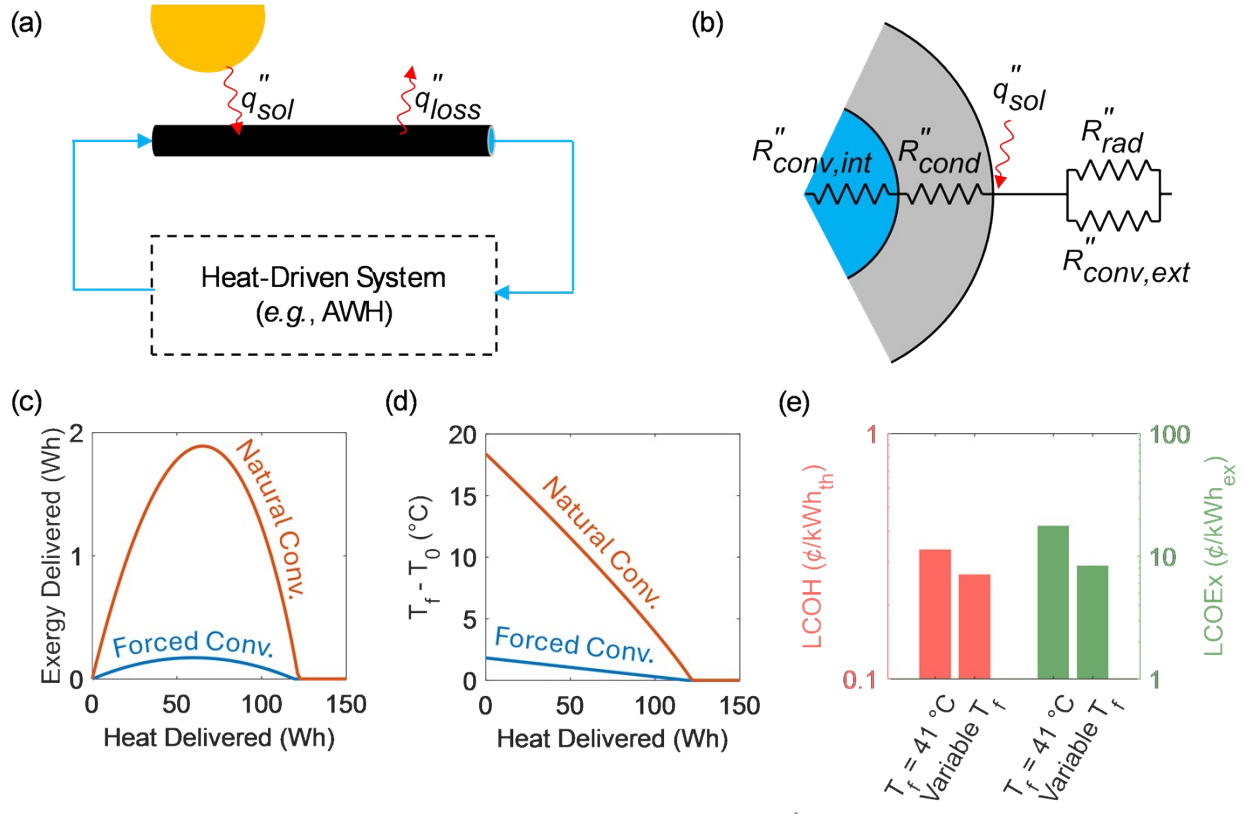

Figure S3. Cheap, low-grade heat source consisting of a pipe painted black, absorbing heat from the sun and transferring it to a heat transfer fluid. (a) System schematic. (b) Thermal resistance network used to solve for the temperature of the heat transfer fluid for each hour of the year; two scenarios are considered – one in which the external convection heat transfer coefficient is determined from the wind speed, and one in which the external convection coefficient is zero (i.e., only radiation losses occur). (c) The exergy delivered by the pipe during a particular 30 minute interval, as a function of the heat delivered. (d) The temperature different between the heat transfer fluid and the ambient for the same 30 minute interval, as a function of the heat delivered. (e) The LCOH (left axis) and LCOEx (right axis) of the pipe when natural convection occurs at the exterior surface.

Figure S3e plots the LCOH and LCOEx of the black pipe. Notably, while the LCOH is very low (< 1 ¢/kWhth), the LCOEx is far higher, due to the small amount of exergy delivered by the very low-grade heat. Realistically, the heat delivery temperature would be approximately fixed at a particular temperature. For example, for sorbent AWH, the heat delivery temperature should be near the desorption temperature of the sorbent; if it is too low, the absorbed moisture will not desorb, and if it is excessively high then no extra moisture will be produced and exergy will be destroyed. The optimal fixed temperature was found to be 41 °C, as this is the fluid temperature that would maximize exergy delivery across the year (and thus minimize LCOEx). At this temperature, the LCOEx becomes 17.7 ¢/kWhex. If the heat delivery temperature is allowed to vary with time, then it could be set each hour to the value that maximizes the exergy delivered to the system. In this case, the LCOEx becomes 8.4 ¢/kWhex. Thus, while the heat from the solar absorber is cheap (low LCOH) due to an ultra-low CAPEX and zero OPEX, the heat has little exergy (due to the low exergy factor), and the LCOEx of solar heater is still higher than that of electricity. This dispels the misconception that energy systems powered by low-grade heat (e.g., AWH systems) will receive heat "for free". It should again be noted that this LCOEx for a pipe painted black is likely generously low, since the estimated production cost of the pipe was used, instead of the retail price. Thus, the LCOEx of a very low-grade solar absorber like the one in Figure S3e will likely be even higher than 17.7 ¢/kWhex.

Figure S3c shows the exergy delivered for a given 30 minute period of the year (12:30 – 1:00 PM local time on July 2nd) as a function of the heat delivered. For zero rate of heat delivery, the temperature of the fluid is at its highest, but no heat is being transferred to the fluid, so no exergy is delivered. At the other extreme, when all of the incident radiation is delivered to the heat transfer fluid (*i.e.*, no losses to the ambient at the external surface), the fluid temperature is at the

ambient temperature, so the heat contains no exergy. Thus, the peak exergy delivered occurs at some rate of heat transfer between these two extremes. This also means that the peak exergy delivered occurs at a different fluid temperature for each time interval throughout the year. As expected, both the exergy delivered to the fluid and the temperature of the fluid increase as when the external surface is exposed to natural convection instead of forced convection.

From the thermal resistance network in Figure S3b, the equation for the temperature of the heat transfer fluid in the pipe, as a function of the heat flux to the fluid, $q_d^{''}$, is given in Eq. (S1).

$$T_f = T_0 + \frac{q_{sol}^{''} - q_d^{''}}{R_{ext,conv}^{''\,-1} + R_{rad}^{''\,-1}} - q_d^{''}\left(R_{conv,int}^{''} + R_{cond}^{''}\right) \tag{S1}$$

In Eq. (S1), $q_{sol}^{''}$ is the rate of heat transfer to the pipe from the sun, normalized by the entire pipe surface area ($\pi \times D \times L$). The rate of heat transfer from the sun to the pipe is equal to the direct normal irradiance multiplied by the projected area ($D \times L$). Thus, $q_{sol}^{''}$ is equal to the direct normal irradiance divided by π. $q_d^{''}$ is the rate of heat transfer to the fluid, normalized by the outer surface area. All thermal resistances are in units of m^2K/W; *i.e.*, the resistances (in K/W) were multiplied by the outer surface area. The internal convection coefficient was calculated using the Dittus-Boelter equation,[11] while the conduction resistance was calculated for the thermal conductivity of aluminum (237 W/m-K) and a pipe wall thickness of 0.047". It was assumed that the pipe behaves as a perfect black body (due to the black paint), so the equation for the convection resistance takes the form in Eq. (S2).

$$R_{rad}^{''} = \left[\sigma\left(T_{ext} + T_0\right)\left(T_{ext}^{\,2} + T_0^2\right)\right]^{-1} \tag{S2}$$

Two scenarios were considered for the external surface of the pipe – one in which forced convection occurred (based on the wind speed during the given time interval) and one in which natural convection occurred. The forced convection coefficient was calculated using the Churchill and Bernstein equation, while the natural convection coefficient was calculated using the Churchill and Chu equation.[11]

The radiation and natural convection resistances are functions of the external surface temperature, which was not initially known, so an iterative scheme was used to find the external surface temperature.

Notably, in our analysis, we assume that the temperature does not vary in the angular direction, even though the irradiation is incident only on a portion of the pipe surface. In other words, we assume that the conduction resistance in the angular direction is negligible at the exterior surface of the pipe (due to the high thermal conductivity of aluminum), which allows the heat transfer analysis to be greatly simplified to a 1D case (in the radial direction).

We assume that the cost of producing a pipe is twice the raw material price of the metal out of which the pipe is made. We consider a 1" outer diameter pipe with 0.047" thickness, which has a volume of 27.67 cm^3 per ft. Based on their densities, a copper pipe of this size would weigh 0.55 lb per ft (247.93 g per ft), while an aluminum pipe would weight 0.16 lb per ft (74.71 g per ft). Based on the raw material prices of metals,[12,13] the copper pipe would cost \$2.22/ft, while the aluminum pipe would cost \$0.19/ft. A 1" outer diameter pipe that has an outer surface area of 1 m^2 would have a length of 41.12 ft. Thus, the areal cost of the raw material in the copper pipe (normalized per unit outer surface area) is \$91.46/m^2, while the areal cost of the raw material of the aluminum pipe is \$7.81/m^2. The aluminum pipe is then chosen due to its lower cost. From the assumption that raw materials account for 50% of the production cost, the pipe cost comes out to

be $15.62/m^2. Notably, this value is ~ 90% less than the retail price per ft of a 1” outer diameter aluminum pipe.[14] Thus, our analysis is very generous towards the technoeconomic performance of a black pipe.

For the cost of a coat of paint, we choose a value of $0.1/ft^2, which is based purely on the material cost of a paint that costs $20/gallon, is 50% solids by volume, and has a layer thickness of 4 mm. This is equal to $1.08/m^2.

Supplementary Note 4: Delineation Between System and Heat Source

When a heat pump is used to drive a thermal process, the system can be described as work-driven or heat-driven, depending on where the system boundary is drawn. This is illustrated in Figure S4 below, where the boundary has been drawn to classify the system as work-driven in Figure S4a and heat-driven in Figure S4b. For the work-driven system in Figure S4a, the overall system exergetic efficiency is 5% (the product of the 50% efficient heat pump and the 10% efficient dehumidifier), the CAPEX of the overall system is 24 ¢ per kWh_{ex} of electricity input (14 ¢ for the heat pump and 10 ¢ for the dehumidifier), and the LCOEx of the energy input is 11 ¢/kWh_{ex} (the retail price of electricity). Meanwhile, for the heat-driven system in Figure S4b, the dehumidifier exergetic efficiency is 10%, the system CAPEX is 20 ¢ per kWh_{ex} of exergy input, and the LCOEx of the low-grade heat input is 50 ¢/kWh_{ex} (which is calculated from the 14 ¢/kWh_{ex} CAPEX and exergetic efficiency of the heat pump, as well as the 11 ¢/kWh_{ex} retail price of electricity). In both cases, the LCOEx of the dehumidifier output is 700 ¢/kWh_{ex}; thus, the drawing of the system boundary is arbitrary for the purpose of calculating the LCOEx of the output and only matters in the context of calculating the LCOEx of the exergy input. The benefit of drawing the separate boundaries in Figure S4b is that it de-couples the heat pump and dehumidifier subsystems and provides more insight into the heat (revealing that the low-grade heat input to the dehumidifier has a high LCOEx). It should be noted that some systems use a vapor compression cycle to simultaneously produce useful cooling at the evaporator and useful heat to regenerate a desiccant at the condenser.[15] In this case, the co-production of two exergy streams, heating and cooling, makes it difficult to quantify the LCOEx of the regeneration heat (*i.e.*, drawing two system boundaries as in Figure S4b), and the system should be classified as electrically-driven (as in Figure S4a).

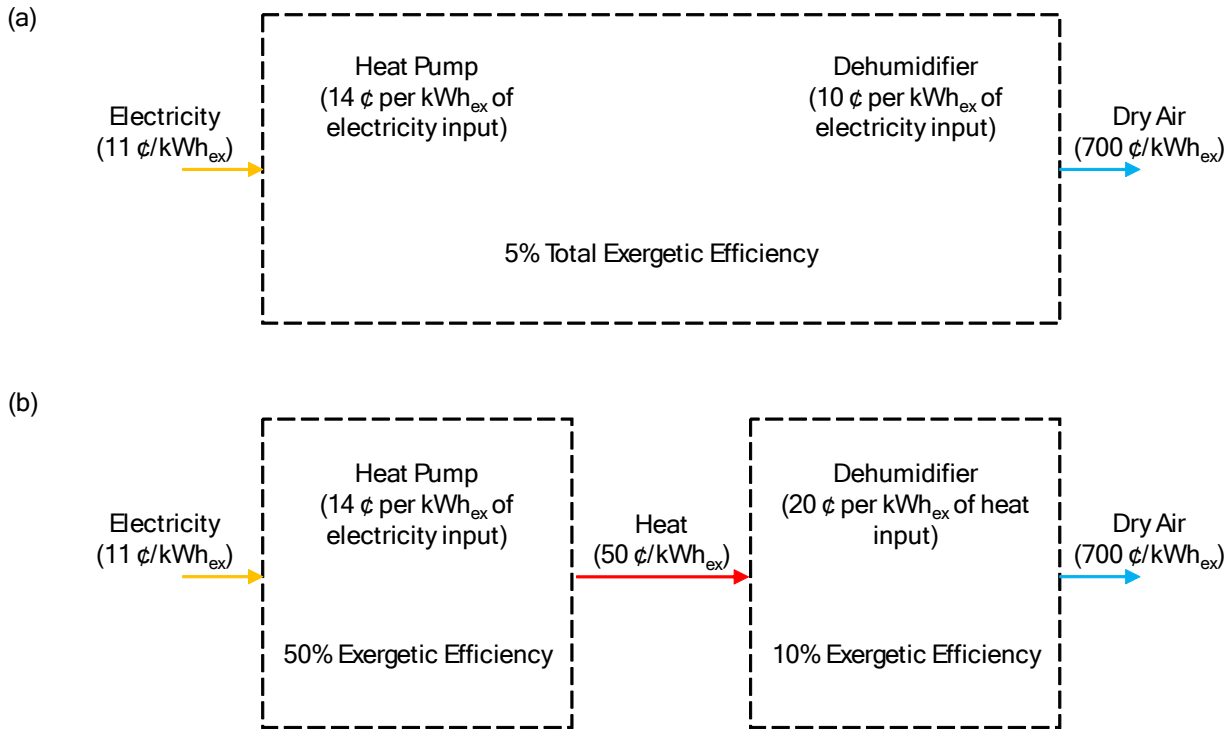

Figure S4. Heat pump-driven dehumidifier with (a) one control volume drawn around both the heat pump and dehumidifier, and (b) two separate control volumes.

Supplementary Note 5: Chemical Exergy of Liquid Water and Sulfur Depolarized Electrolysis

The exergy of pure liquid water at ambient temperature and pressure is equal to the difference between the chemical potential of the pure water and the water in the reference environment, as given in Eq. (S3).

$$ex_w = \mu_{w,pure}(T_{amb},P_{amb}) - \mu_{w,ref}(T_{amb},P_{amb}) \quad \text{(S3)}$$

The chemical potential of water in an aqueous mixture at the reference temperature and total pressure is given in Eq. (S4), where a_w is the water activity of the mixture.

$$\mu_w(T_{ref},P_{ref}) = RT_{amb}\ln(a_w) \quad \text{(S4)}$$

In Figure 1 of the main text, the reference environment is seawater with a water activity of 0.97 and a temperature of 300 K. Thus, the exergy of the pure water equates to 4.2 kJ/kg, as given in Eq. (S5). Multiplying by the flowrate of 1 kg/s gives a rate of exergy flow of 4.2 kW for the pure water.

$$ex_w = RT_{amb}\ln(1/0.97) = 4.2\ kJ/kg \quad \text{(S5)}$$

Meanwhile, in arid regions, the water activity of ambient air can be as low as 0.12 (*i.e.*, 12% relative humidity).[16] In a dry location like this, Eq. (S4) reveals that the exergy of liquid water relative to ambient air is ~ 80 kWh_{ex}/m^3 (which is equal to the theoretical minimum specific energy consumption of atmospheric water harvesting in such a location).

The chemical exergy balance of conventional and sulfur depolarized electrolysis can also be determined. The reaction formula for conventional electrolysis is given in Eq. (S7).

$$H_2O \rightarrow H_2 + \frac{1}{2}O_2 \tag{S7}$$

Based on the chemical exergies from Szargut,[17] the chemical exergy of liquid H_2O is ~ 0 kJ_{ex}/mol, while H_2 is 236.09 kJ_{ex}/mol, and O_2 is 3.97 kJ_{ex}/mol. Then, this reaction requires ~ 238.08 kJ_{ex} of energy input to produce 1 mol of H_2. If both H_2 and O_2 are useful products of the process, then the output specific chemical exergy is 13.21 kJ_{ex} per g of product. If the O_2 is discarded, then the output specific chemical exergy is 117.11 kJ_{ex} per g of product. Thus, conventional electrolysis produces a high-exergy output, which leads to a high specific cost of the product (H_2). Meanwhile, the reaction formula for sulfur depolarized electrolysis is given in Eq. (S8).

$$2H_2O + SO_2 \rightarrow H_2 + H_2SO_4 \tag{S8}$$

Based on the chemical exergies from Szargut,[17] the chemical exergy of SO_2 is 313.4 kJ_{ex}/mol, while H_2SO_4 is 163.4 kJ_{ex}/mol. Then, this reaction requires only ~ 86.09 kJ_{ex} of energy input to produce 1 mol of H_2, while simultaneously producing 1 mol of H_2SO_4. Furthermore, the specific chemical exergy of the co-produced hydrogen and sulfuric acid output is merely 3.99 kJ_{ex} per g of product. Because of the low specific exergy of the output, the product will have a low specific cost.

Supplementary Note 6: Other Electrically-Driven Regime Maps

Along with the electrically-driven regime maps in Figure 6 of the main text, we provide two more applications here. The first is for transportation, with the LCOEx of gasoline compared to that of electricity + a Li-ion battery in Figure S5. With current electricity costs (Figure S5a) and battery CAPEX, the LCOEx of the battery electric vehicle (BEV) is more expensive than gasoline. Meanwhile, if low-cost electricity is used (Figure S5b), the LCOEx of the BEV is on-par with gasoline. Reduction in battery CAPEX could bring the LCOEx of the BEV below that of gasoline.

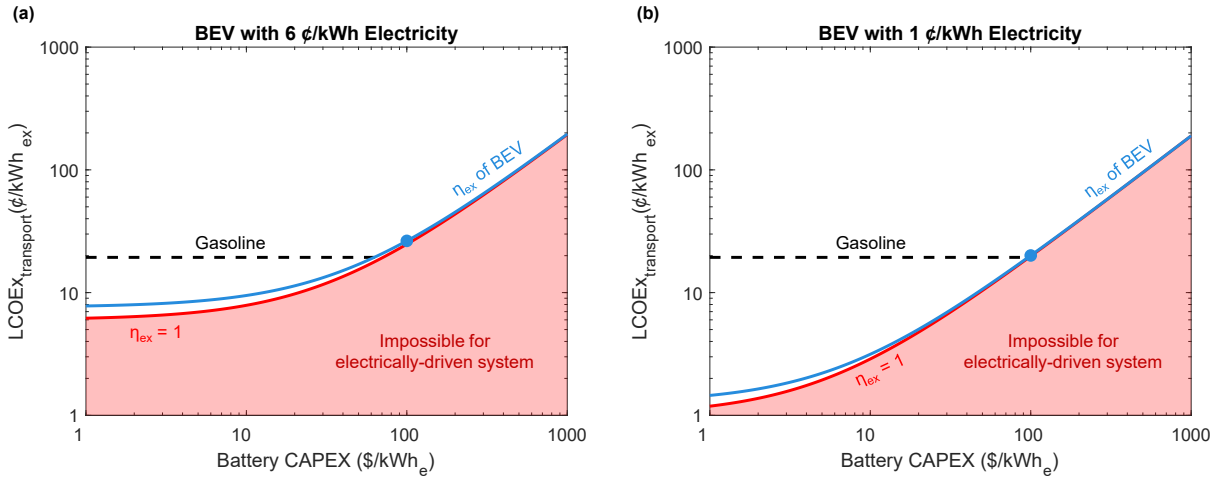

Figure S5. Transportation LCOEx regime maps, with (a) current electricity prices, and (b) cheap electricity.

The second application presented here is dehumidification, with the LCOEx plotted in Figure S6. For current dehumidification, we assume a CAPEX of $5 per pint/day.[18] The exergetic efficiency of current dehumidifiers varies widely by technology and outdoor conditions; to choose a representative value, we use the Energy Star standard integrated energy factor of 3.3 L/kWh,[19] which is equivalent to a specific exergy consumption of 0.3 kWh_{ex}/kg. This standard is independent of outdoor conditions,[20] but it corresponds to an exergetic efficiency of 7.6% when

the indoor dew point temperature is 55 °F and the outdoor dew point temperature is 72 °F (representative conditions for a location where dehumidification is required). For electricity, we used a value of 10 ¢/kWh$_e$, which is representative of the residential and commercial sectors. From Figure S6, dehumidifiers currently produce dry air with a very high LCOEx. Improvements in exergetic efficiency and reductions in CAPEX have the potential to significantly reduce the output LCOEx of dehumidification.

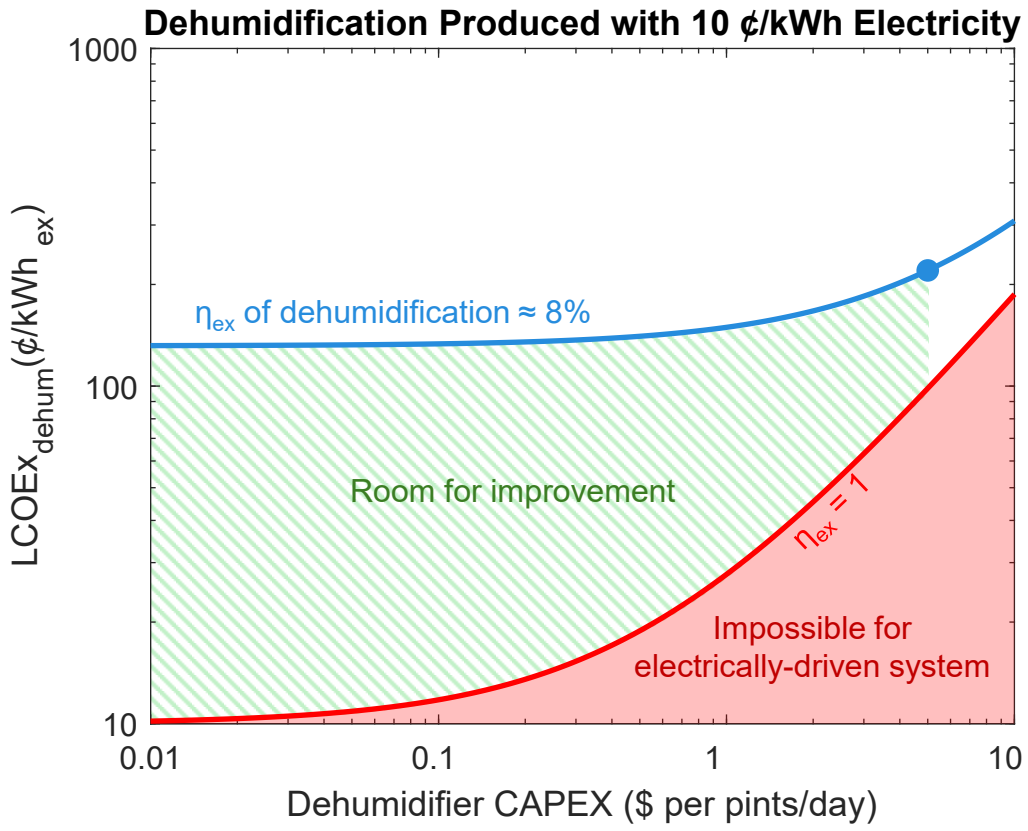

Figure S6. LCOEx regime map for dehumidification.

References

1 A. S. Reimers and M. E. Webber, *Texas Water Journal*, 2018, **9**, 82–95.
2 A. K. Menon, M. Jia, S. Kaur, C. Dames and R. S. Prasher, *iScience*, 2023, **26**, 105966.
3 A. Mahfouz, A. Z. Haddad, J. D. Kocher and A. K. Menon, *Journal of Materials Chemistry A*, 2025, **13**, 275–288.
4 A. Z. Haddad, A. K. Menon, H. Kang, J. J. Urban, R. S. Prasher and R. Kostecki, *Environ. Sci. Technol.*, 2021, **55**, 3260–3269.
5 Y. Cai, W. Shen, J. Wei, T. H. Chong, R. Wang, W. B. Krantz, A. G. Fane and X. Hu, *Environ. Sci.: Water Res. Technol.*, 2015, **1**, 341–347.
6 J. D. Kocher, S. K. Yee and R. Y. Wang, *Energy Conversion and Management*, 2022, **253**, 115158.
7 F. Zhao, X. Zhou, Y. Liu, Y. Shi, Y. Dai and G. Yu, *Advanced Materials*, 2019, **31**, 1806446.
8 J. D. Kocher, A. K. Menon and S. K. Yee, American Society of Mechanical Engineers Digital Collection, 2023.
9 X. Li, B. El Fil, B. Li, G. Graeber, A. C. Li, Y. Zhong, M. Alshrah, C. T. Wilson and E. Lin, *ACS Energy Lett.*, 2024, **9**, 3391–3399.
10 A. LaPotin, Y. Zhong, L. Zhang, L. Zhao, A. Leroy, H. Kim, S. R. Rao and E. N. Wang, *Joule*, 2021, **5**, 166–182.
11 Y. A. Çengel and A. J. Ghajar, *Heat and mass transfer: fundamentals & applications*, McGraw Hill Education, New York, NY, Fifth edition., 2015.
12 Precious and Industrial Metals, https://www.bloomberg.com/markets/commodities/futures/metals, (accessed December 21, 2024).
13 Daily Metal Price: Aluminum Price (USD / Pound) Chart for the Last Year, https://www.dailymetalprice.com/metalpricecharts.php?c=al&u=lb&d=240, (accessed December 21, 2024).
14 Aluminum Quick-Connect Pipe for Compressed Air, https://www.mcmaster.com/, (accessed December 23, 2024).
15 J. Woods, E. Kozubal, P. Luttik, D. Fox and J. Warner, *Modeling and Experiments on a Dedicated Outdoor Air System Using Liquid Desiccant Heat and Mass Exchangers*, West Lafayette, IN: Purdue University, 2022.
16 J. D. Kocher and A. K. Menon, *Energy Environ. Sci.*, 2023, **16**, 4983–4993.
17 J. Szargut, *Egzergia : poradnik obliczania i stosowania*, Wydawnictwo Politechniki Śląskiej, 2007.
18 Waykar 50 Pint Energy Star Dehumidifier with Pump for Basement, 7000 Sq. Ft, Auto Defrost, Self-Drying, Ultra Quiet, https://www.walmart.com/ip/50-Pint-Energy-Star-Dehumidifier-Home-Basement-Large-Room-7000-Sq-Ft-Max-150-Pint-Pump-Auto-Defrost-Self-Drying-System-Dual-Drain-Hose-Tank-Ultra-Qui/16863404913, (accessed July 10, 2025).
19 Dehumidifiers Key Efficiency Criteria | ENERGY STAR, https://www.energystar.gov/products/dehumidifiers/key_efficiency_criteria, (accessed July 10, 2025).
20 Appendix X1 to Subpart B of Part 430, Title 10 -- Uniform Test Method for Measuring the Energy Consumption of Dehumidifiers, https://www.ecfr.gov/current/title-10/appendix-Appendix%20X1%20to%20Subpart%20B%20of%20Part%20430, (accessed July 10, 2025).